



Título artículo / Títol article:

Effects of green space spatial pattern on land surface temperature: Implications for sustainable urban planning and climate change adaptation

Autores / Autors

Maimaitiyiming, Matthew ; Ghulam, Abduwasit ; Tiyip, Tashpolat ; Pla Bañón, Filiberto ; Latorre Carmona, Pedro ; Halik, Ümüt ; Sawu, Mamat ; Caetano, Mario

Revista:

ISPRS Journal of Photogrammetry and Remote Sensing

Versión / Versió:

Postprint

Cita bibliográfica / Cita bibliogràfica (ISO 690):

MAIMAITIYIMING, Matthew, et al. Effects of green space spatial pattern on land surface temperature: Implications for sustainable urban planning and climate change adaptation. ISPRS Journal of Photogrammetry and Remote Sensing, 2014, vol. 89, p. 59-66.

url Repositori UJI:

<http://hdl.handle.net/10234/135506>

1
2
3
4 1 **Effects of green space spatial pattern on land surface temperature:**

5
6
7 2 **implications for sustainable urban planning and climate change adaptation**

8
9
10 3
11
12 4 Matthew Maimaitiyiming^a, Abduwasit Ghulam^a, Tashpolat Teyip^{b,c}, Filiberto Pla^d, Pedro

13
14
15 5 Latorre-Carmona^d, Mário Caetano^e, Mamat Sawut^{a,b,c}, Ümüt Halik^{b,c}

16
17 6
18
19
20 7 ^a Center for sustainability, Saint Louis University, Saint Louis, MO 63103, USA

21
22 8
23
24 9 ^b College of Resources and Environmental Sciences, Xinjiang University, Urumqi, Xinjiang

25
26
27 10 830046, China

28
29
30 11
31
32 12 ^c Ministry of Education Key Laboratory of Oasis Ecology at Xinjiang University, Urumqi,

33
34 13 Xinjiang 830046, China

35
36
37 14
38
39 15 ^d Institute of New Imaging Technologies, University Jaume I, 12071 Castellón, Spain

40
41 16
42
43
44 17 ^e Institute for Statistics and Information Management (ISEGI), Universidade Nova de Lisboa,

45
46 18 Campus de Campolide, 1070-312, Lisboa, Portugal

47
48
49 19
50
51
52 20
53
54 21 **Abstract**—The urban heat island (UHI) refers to the phenomenon of higher atmospheric
55
56 22 and surface temperatures occurring in urban areas than in the surrounding rural areas. Mitigation
57
58
59 23 of the UHI effects via the configuration of green spaces and sustainable design of urban

1
2
3
4
5
6
7
8
9
10
11
12
13
14
15
16
17
18
19
20
21
22
23
24
25
26
27
28
29
30
31
32
33
34
35
36
37
38
39
40
41
42
43
44
45
46
47
48
49
50
51
52
53
54
55
56
57
58
59
60
61
62
63
64
65

24 environments has become an issue of increasing concern under changing climate. In this paper,
25 the effects of the composition and configuration of green space on land surface temperatures
26 (LST) were explored using landscape metrics including percentage of landscape (PLAND), edge
27 density (ED) and patch density (PD). An oasis city of Aksu in Northwestern China was used as a
28 case study. The metrics were calculated by moving window method based on a green space map
29 derived from Landsat Thematic Mapper (TM) imagery, and LST data were retrieved from
30 Landsat TM thermal band. Normalized mutual information measure was employed to investigate
31 the relationship between LST and the spatial pattern of green space. The results showed that
32 while the PLAND is the most important variable that elicits LST dynamics, spatial configuration
33 of green space also has significant effect on LST. Though, the highest normalized mutual
34 information measure was with the PLAND (0.71), it was found that ED and PD combination is
35 the most deterministic factors of LST than the unique effects of a single variable or the joint
36 effects of PLAND and PD or PLAND and ED. Normalized mutual information measure
37 estimations between LST and PLAND and ED, PLAND and PD and ED and PD were 0.7679,
38 0.7650 and 0.7832, respectively. A combination of the three factors PLAND, PD and ED
39 explained much of the variance of LST with a normalized mutual information measure of
40 0.8694. Results from this study can expand our understanding of the relationship between LST
41 and street trees and vegetation, and provide insights for sustainable urban planning and
42 management under changing climate.

43
44
45 **Keywords**—urban heat island, urban green space, landscape metrics, configuration, normalized
46 mutual information measure.

1. Introduction

The urban heat island (UHI) refers to the phenomenon of higher atmospheric and surface temperatures occurring in urban areas than in the surrounding rural areas. This phenomenon is widely observed in cities regardless of their sizes and locations (Connors et al., 2013; Cui and de Foy, 2012; Imhoff et al., 2010; Li et al., 2012; Tran et al., 2006). The UHI is mainly caused by the modification of land surfaces by urban development, which uses materials that effectively store short-wave radiation (Solecki et al., 2005). As the result, land surface temperature (LST) increases due to the UHI, which may disrupt species composition and distribution (Niemelä, 1999) by increasing the length of growing seasons, decrease air quality (Feizizadeh and Blaschke, 2013; Lai and Cheng, 2009; Sarrat et al., 2006; Weng and Yang, 2006), leading to greater health risks (Patz et al., 2005). The UHI may also decrease water quality as warmer waters flow into streams putting additional stress on aquatic ecosystems (James, 2002). Therefore, it has become a major research focus in urban climatology and urban ecology since first reported in 1818 (Howard, 1818).

The intensity and spatial pattern of UHI are largely exacerbated from population dynamics and development of build-up areas (Arnfield, 2003; Wu et al., 2013). Specifically, urban structure (e.g. height-to-width ratio of buildings and streets), , proportion of built-up versus green spaces per unit area, weather conditions (e.g. wind and humidity), and socioeconomic activities determine the development of the UHI (Hamdi and Schayes, 2007; Rizwan et al., 2008b; Taha, 1997; Unger, 2004; Voogt and Oke, 1998). For example, Huang et al. (2011) found statistically significant relationship between the UHI and socioeconomic factors indicating that a higher UHI effects were linked to block groups characterized by low income, high poverty, less education, more ethnic minorities, more elderly people and greater risk of

1
2
3
4 70 crime. As many of these factors, especially land surface characteristics are primarily represented
5
6
7 71 by land-cover and land-use (LCLU), the relationship between the LST and LCLU has been the
8
9 72 focus of numerous studies on the UHI (Buyantuyev and Wu, 2010; Dousset and Gourmelon,
10
11 73 2003; Pu et al., 2006; Voogt and Oke, 2003;Weng et al., 2004). This is due to the fact that
12
13
14 74 vegetation usually has higher evapotranspiration and lower emissivity than built-up areas, and
15
16 75 thus has lower surface temperatures (Hamada and Ohta, 2010; Weng et al., 2004).

17
18
19 76 Composition and configuration of green spaces are the two major elements of LCLU. The
20
21 77 former refers to the abundance and variety of land cover types and the latter is related to the
22
23 78 spatial arrangements and layout of land cover types (Connors et al., 2013; Turner, 2005).
24
25
26 79 Remarkable proliferations of studies focusing on the relationship between LST and green space
27
28 80 composition has been reported over the last two decades (Chen et al., 2006; Tran et al., 2006;
29
30
31 81 Voogt and Oke, 2003; Weng, 2009; Weng et al., 2004). Though the magnitude of correlations
32
33 82 varied among these reports, a negative relationship between the vegetation amount/fraction and
34
35
36 83 LST was consistently observed. However, the spatial characteristics and configurations of
37
38 84 vegetation patches within the urban environment have significant impacts on the distribution of
39
40
41 85 the UHI (Bowler et al., 2010; Cao et al., 2010; Honjo and Takakura, 1991; Yokohari et al., 1997;
42
43 86 Zhao et al., 2011), and that the size and shape of a vegetation patch creates cool island effects, a
44
45
46 87 phenomenon that the temperature of green space is lower than its surrounding areas (Cao et al.,
47
48 88 2010; Zhang et al., 2009). Based on a case study of a heavily urbanized Beijing metropolitan
49
50
51 89 area in China, Li et al. (2012) also indicated that increasing patch density results in significantly
52
53 90 higher LST when the size of urban green space unaffected, and that spatial configuration has a
54
55 91 significant influence in the variability of derived LST.

1
2
3
4
5
6
7
8
9
10
11
12
13
14
15
16
17
18
19
20
21
22
23
24
25
26
27
28
29
30
31
32
33
34
35
36
37
38
39
40
41
42
43
44
45
46
47
48
49
50
51
52
53
54
55
56
57
58
59
60
61
62
63
64
65

92 It is evident from an exhaustive literature review hitherto that there is a lack of case
93 studies within arid regions (Connors et al., 2013). As cities are growing fast in population, and
94 urbanization is projected to be high (Baker et al. 2004), sustainable planning of urban
95 environment to mitigate UHI effects highlights a pressing need for immediate attention. This is
96 further emphasized by climate changes as arid regions are likely to become even drier in
97 response to increasing temperature from global warming (Durack et al., 2012). Driven by fast
98 economic growth and population increase, Northwestern China has experienced rapid
99 urbanization in the past several decades, along with a drastic transformation of the urban
100 environment and social equity (Fan and Qi, 2010; Halik et al., 2013; Liu et al., 2013). In
101 addition, the majority of the previous studies used ordinary least squares regression and/or spatial
102 autoregression to analyze the relationship between the landscape metrics and LST. The statistical
103 significance of the relationship between the landscape metrics and LST varied between the
104 methods (Li et al., 2012). Comparative approaches with additional case studies are needed to
105 generalize the methods and concepts demonstrated by these preliminary attempts. To that end,
106 we investigate the effects of composition and configuration of urban green space on LST using a
107 robust moving window algorithm of normalized mutual information measure in the arid city of
108 Aksu, Xinjiang Uyghur Autonomous Region in Northwestern China. One of the advantages of
109 using mutual information measures is that it can capture linear as well as strongly non-linear
110 relationships among variables under the “umbrella” of just one concept (“mutual information”).
111 The goal is to provide guiding suggestions for sustainable urban planning and development
112 under future climate changes. We chose to use Landsat 30 m resolution data as previous studies
113 (Liu and Weng, 2009; Li et al., 2013) have demonstrated that 30 m and 90 m are the optimal

1
2
3
4
5
6
7
8
9
10
11
12
13
14
15
16
17
18
19
20
21
22
23
24
25
26
27
28
29
30
31
32
33
34
35
36
37
38
39
40
41
42
43
44
45
46
47
48
49
50
51
52
53
54
55
56
57
58
59
60
61
62
63
64
65

114 resolutions to study the relationship between LST and landscape patterns at patch level and
115 landscape levels, respectively.

116 The paper is organized in the sections below. Following the description of the study area in
117 Section 2, the methodology of calculating LST, landscape metrics, and a brief introduction to
118 normalized mutual information measure are presented in Section 3. The results, discussions and
119 conclusions are presented in Section 4, 5 and 6, respectively.

120

121 2. Study area

122

123 The study area, downtown Aksu City, Northwestern China, is a typical oasis city located in an
124 arid region. Aksu City is the capital of Aksu Prefecture in Xinjiang Uyghur Autonomous Region,
125 China. Geographically, the city is situated in south of the Tianshan Mountains and northwest
126 edge of the Tarim Basin (39°30'N - 41°27'N, 79°39'E - 82°01'E; Fig. 1). Aksu City is known as
127 “the Land of Melons and Fruits”. It includes municipal total area of 14,300 Km² and built-up area
128 of 28.1 Km².

129

130 Aksu City is rich in light and heat resources. It has a long frost-free period from 205 to 219 days.
131 The climate is dry, and rainfall is extremely rare with less than 50 mm per year and average
132 annual evaporation of 1950 mm. Topography of the study area is flat. The climatic and the
133 physiographic conditions are mostly the same across the region. Therefore, it is an ideal area to
134 explore the relationship between LST and spatial pattern of green space in arid and semi-arid
135 land.

136

1
2
3
4
5
6
7
8
9
10
11
12
13
14
15
16
17
18
19
20
21
22
23
24
25
26
27
28
29
30
31
32
33
34
35
36
37
38
39
40
41
42
43
44
45
46
47
48
49
50
51
52
53
54
55
56
57
58
59
60
61
62
63
64
65

137 The proportion of green area in the metropolitan region has increased to 30.6% today from 12 %
138 in early 1980s. Urban green space coverage has reached 39.2% with the per capita public green
139 area of 9 m². Meanwhile, city's ecological environment has been significantly improved. This
140 rapid growth in green space emphasizes a need to develop most effective configuration of green
141 space to reduce the urban heat island caused by expanding impervious surfaces and to adapt to
142 the global climate change.

Insert Figure 1 here

147 3. Methodology

148 3.1. Land Surface Temperature

149 Landsat-5 Thematic Mapper (TM) thermal infrared band 6 (11.45 – 12.50μm) data with 120 ×
150 120 m resolution were utilized to derive the LST (Fig. 2b). The satellite data were collected on
151 August 19, 2011, which was a clear day with 0 % cloud cover. Meteorological variables that
152 influence the intensity of urban heat environment at the time of image capture were obtained
153 from China standard meteorological station in the study site. These variables include daily
154 precipitation (0 mm), daily average wind speed (1.6 m/s), wind direction (South-East) and
155 humidity (46 %). Due to the lack of detailed in-situ atmospheric variables that allow physical
156 inversion of brightness temperature to LST, a mono-window algorithm was applied for retrieval
157 of LST (Qin et al., 2001)

$$159 T_s = [a(1 - C - D) + (b(1 - C - D) + C + D)]T_{sensor} - DT_a \quad (1)$$

1
2
3
4
5
6
7
8
9
10
11
12
13
14
15
16
17
18
19
20
21
22
23
24
25
26
27
28
29
30
31
32
33
34
35
36
37
38
39
40
41
42
43
44
45
46
47
48
49
50
51
52
53
54
55
56
57
58
59
60
61
62
63
64
65

161 With $C = \varepsilon\tau$, $D = (1 - \tau)[1 + (1 - \varepsilon)\tau]$, $a = -67.355351$ and $b = 0.458606$, where ε land surface
162 emissivity (LSE) is, τ is the total atmospheric transmissivity, T_{sensor} is the at-sensor brightness
163 temperature, and T_a represents the mean atmospheric temperature given by:

$$T_a = 16.011 + 0.92621T_0 \quad (2)$$

167 With T_0 being the near-surface air temperature. Qin et al. (Qin et al., 2001) also estimated the
168 atmospheric transmissivity from w , the atmospheric water vapor content, for the range 0.4 to 1.6
169 g/cm^2 , according to the following equations:

$$\tau = 0.97429 - 0.08007 w, \text{ and} \quad (3)$$

$$\tau = 0.982007 - 0.09611 w \quad (4)$$

174 Both T_0 and w were obtained from local meteorological stations. LSE was obtained from the
175 NDVI thresholds method (Sobrino et al., 2004).

$$\varepsilon = \varepsilon_{soil}, \text{ when } NDVI < 0.2, \quad (5)$$

$$\varepsilon = \varepsilon_{veg}, \text{ when } NDVI > 0.5 \text{ and} \quad (6)$$

$$\varepsilon = \varepsilon_{veg}P_v + d\varepsilon, \text{ when } 0.2 \geq NDVI \geq 0.5, \quad (7)$$

181 where ε_{soil} is the soil emissivity, ε_{veg} is the vegetation emissivity, and $d\varepsilon$ includes the effects of
182 the geometry of natural surfaces and the internal reflections. Because most of the study area is a

1
2
3
4 183 plain surface, this term is negligible. P_v is the fraction of the vegetation that can be computed by
5
6
7 184 the following formula (Carlson and Ripley, 1997).
8

$$P_v = \left[\frac{NDVI - NDVI_{\min}}{(NDVI_{\max} - NDVI_{\min})} \right]^2 \quad (8)$$

9 185
10
11
12 186
13
14
15
16 187
17
18
19 188 where, $NDVI_{\max} = 0.5$, and $NDVI_{\min} = 0.2$. Soil and vegetation emissivities were estimated to be
20
21
22 189 0.97 and 0.99, respectively (Sobrino et al., 2004).
23
24 190
25
26

27 191 *3.2. Spatial Pattern of Green Space*

28
29 192
30
31
32 193 The multi-spectral Landsat-5 TM data acquired on August 19, 2011 were used to map green
33
34 194 space (i.e., vegetated areas) (Fig. 2a). The spatial resolution of the multispectral data is 30 m. A
35
36
37 195 maximum likelihood image classification approach was applied to extract the vegetated area
38
39 196 using ENVI from EXELIS Visual Information Solutions. The four bands green, red, near-
40
41
42 197 infrared, and two shortwave infrared were used for classification. An accuracy assessment was
43
44 198 conducted based on 200 ground reference data that were photo interpreted from existing land
45
46
47 199 cover map with a scale of 1:150000 (produced by Land Resources Bureau of Aksu City and
48
49 200 College of Resources and Environmental Sciences, Xinjiang University, China in June, 2012)
50
51 201 together with Landsat true color image. The overall accuracy of the derived classification map
52
53
54 202 was 87.60 %, and the kappa coefficient was 0.83 (Table 1).
55
56

1
2
3
4
5
6
7
8
9
10
11
12
13
14
15
16
17
18
19
20
21
22
23
24
25
26
27
28
29
30
31
32
33
34
35
36
37
38
39
40
41
42
43
44
45
46
47
48
49
50
51
52
53
54
55
56
57
58
59
60
61
62
63
64
65

205
206
207
208
209
210
211
212
213
214
215
216
217
218
219
220
221
222
223
224
225
226
227

Insert Figure 2 here

Insert Table 1 here

It has been demonstrated that land surface temperature or surface urban heat island could be related to LCLU types (Chen et al., 2006; Connors et al., 2013; Weng, 2001; Xian and Crane, 2006), and there are relationships between spatial structure of urban thermal patterns and urban surface characteristics (Li et al., 2011; Liu and Weng, 2008; Weng et al., 2007). The last several decades have witnessed a remarkable proliferation of studies on developing landscape metrics 1) to characterize landscape patterns and its association to UHIs (Gustafson, 1998; Li and Reynolds, 1993; Li and Wu, 2004; McGarigal and Marks, 1995; Turner, 2005; Turner et al., 1989; Wu, 2000; Wu et al., 2002), and 2) to relate landscape patterns to ecological processes (Turner, 2005). With respect to the measurement objectives, these metrics can be generalized into landscape composition and spatial configuration metrics (Gustafson, 1998; McGarigal and Marks, 1995). Landscape composition metrics measure the presence and amount of different patch types within the landscape without explicitly describing its spatial features while landscape configuration metrics measure the spatial distribution of patches within the landscape (Alberti, 2005). In this study, we selected three commonly occurring landscape metrics to relate LST with spatial pattern of urban green space according to the following principles (Lee et al., 2009; Li and Wu, 2004; Riitters et al., 1995; Riva-Murray et al., 2010): (1) important in both theory and practice, (2) easily calculated, (3) interpretable, and (4) minimal redundancy. Table 2 shows the three landscape metrics. See Mcgarigal et al. (2002) for detailed calculation equation and comments. They are selected to provide complementary information about landscape structure for both composition and configuration.

1
2
3
4 228 Insert Table 2 here
5
6
7 229
8
9 230

10 The metrics were calculated using the landscape structure analysis program
11 FRAGSTATS (<http://www.umass.edu/landeco/research/fragstats/fragstats.html>). The
12 231 FRAGSTATS software allows the option of conducting a local structure gradient or moving
13
14 232 FRAGSTATS software allows the option of conducting a local structure gradient or moving
15
16 233 window analysis, and generating the results as a new grid for each selected metric. Our choice
17
18
19 234 was to use moving window analysis, which requires a user specifies the level of heterogeneity
20
21 235 (class or landscape) and the shape (round, square or hexagon) and size (radius or length of side,
22
23
24 236 in meters) of the window to be used. A window of the specified shape and size is passed over all
25
26 237 positively valued cells inside the landscape of interest. However, only cells in which the entire
27
28
29 238 window is contained within the landscape are evaluated. Within each window, the selected
30
31 239 metric at the class or landscape level is computed, and the value is returned to the focal cell. The
32
33
34 240 moving window is passed over the grid until every positively valued cell containing a full
35
36 241 window is assessed in this manner.

37
38 242
39
40
41 243 In our case, we used 8-cell rule which considers all eight adjacent cells that share a side with the
42
43 244 focal cell and 500 m-radius circular window. The window moves over the landscape one cell at
44
45
46 245 a time, calculating the selected metric within the window and returning that value to the center
47
48 246 cell and output a new continuous surface grid map for each selected metric (Mcgarigal et al.,
49
50 247 2002) .
51
52

53 248
54
55
56 249 *3.3. Statistical Correlation Measures*
57
58 250
59
60
61
62
63
64
65

1
2
3
4
5
6
7
8
9
10
11
12
13
14
15
16
17
18
19
20
21
22
23
24
25
26
27
28
29
30
31
32
33
34
35
36
37
38
39
40
41
42
43
44
45
46
47
48
49
50
51
52
53
54
55
56
57
58
59
60
61
62
63
64
65

251 Scatter plots were generated to explore the bivariate relationship between LST and each of the
252 landscape metrics. The normalized mutual information measure was assessed based on them
253 (Cover and Thomas, 1991; Webb, 2002). The Shannon entropy of a continuous random variable
254 X with probability density function $p(x)$ for all possible events $x \in S$ is defined as

$$H(X) = - \int_S p(x) \log p(x) dx \quad (9)$$

255
256 where S is the support of the variable and $p(x)$ is its probability distribution function. Probability
257 distributions may be used to construct a frequency distribution of certain events occurring either
258 discretely, in the form of a histogram, or continuously (Allaby, 2008).

260 In the case of a discrete random variable X , entropy $H(X)$ is expressed as

$$H(X) = - \sum_{x \in \Omega} p(x) \log p(x) \quad (10)$$

264 where $p(x)$ represents the probability of an event $x \in \Omega$ from a finite set (Ω) of possible values.

266 In probability and information theories, the mutual information of two random
267 variables is a quantity that measures the amount of information that both variables share.

268 Formally, the mutual information of two discrete random variables X and Y can be defined as:

$$I(X, Y) = \sum_{x \in X} \sum_{y \in Y} p(x, y) \log \left(\frac{p(x, y)}{p(x)p(y)} \right) \quad (11)$$

1
2
3
4 270
5
6
7 271
8
9 272
10
11
12 273
13
14 274
15
16 275
17
18
19 276
20
21 277
22
23
24 278
25
26 279
27
28
29 280
30
31 281
32
33
34 282
35
36 283
37
38
39 284
40
41 285
42
43 286
44
45
46 287
47
48
49
50
51
52 288
53
54
55 289
56
57 290
58
59
60 291
61
62
63
64
65

where $p(x, y)$ is the joint probability function of X and Y , defined as

$$p(x, y) = P(X = x \& Y = y) \quad (12)$$

We can define:

$$p(x) = \sum_{y \in A} p(X = x, y) \quad (13)$$

$$p(y) = \sum_{x \in A} p(x, Y = y) \quad (14)$$

as the marginal probability distribution functions of X and Y respectively.

$I(x, y)$ is always a non-negative quantity, being zero when the variables are statistically independent. The higher the value of I , the higher is the dependence between them.

The normalized mutual information (Cover and Thomas, 1991; Sridhar et al., 1998), can be defined as

$$C_{XY} = \frac{I(X; Y)}{H(Y)} \text{ and } C_{YX} = \frac{I(X; Y)}{H(X)} \quad (15)$$

This expression can be used as a “correlation” measure (Cover and Thomas, 1991) with the advantage of capturing linear and non-linear relationships among variables. It is sometimes called as “asymmetric dependency coefficient (ADC)” (Sridhar et al., 1998). However, two

1
2
3
4 292 definitions in Eq. (15) will produce unequal values due to their asymmetric property in the
5
6
7 293 definitions. Therefore, a symmetric normalized mutual information measure can be proposed
8
9 294 (Press et al., 1990; Strehl and Ghosh, 2003), such as

$$NI(X, Y) = 2 \frac{I(X, Y)}{H(Y) + H(X)}, NI(X, Y) = \frac{I(X, Y)}{\sqrt{H(Y)H(X)}} \quad (16)$$

10
11 295
12
13
14
15
16
17
18 296
19
20
21 297 It is worth mentioning that the mutual information of two random variables $I(X, Y)$ is always
22
23 298 smaller than the entropy of any of them, i. e., $H(X)$ or $H(Y)$, namely: $I(X; Y) < H(Y)$ and
24
25 299 $I(X; Y) < H(X)$ are valid, because the information both variables share can never be greater than
26
27
28 300 the information each one has. Therefore $0 \leq C_{XY} \leq 1$. If C_{XY} equals one, it means X, Y are
29
30
31 301 perfectly correlated. If C_{XY} equals 0 it indicates there is no correlation between X, Y .

32
33 302
34
35 303 In this study, Eq. 15 was applied to measure the normalized mutual information between the
36
37
38 304 different variables since the focus of the work is to find out the correlation between the land
39
40 305 surface temperature, which is chosen as a proxy of target variable, and other variables including
41
42
43 306 PLAND, PD and ED.

46 307 **4. Results**

47
48 308
49
50 309 The spatial distribution of PLAND is shown in (Fig. 3a), PD (Fig. 3b) and ED (Fig. 3c). Higher
51
52
53 310 vegetation cover or percent green space is located on the eastern edge of the study site, which is
54
55
56 311 possibly a park or a nursery with mature grown trees (Fig. 3a). Patch density is high over the
57
58 312 Middle-Western Aksu downtown (Fig. 3b) indicating more fragmented but evenly distributed
59
60
61
62
63
64
65

1
2
3
4
5
6
7
8
9
10
11
12
13
14
15
16
17
18
19
20
21
22
23
24
25
26
27
28
29
30
31
32
33
34
35
36
37
38
39
40
41
42
43
44
45
46
47
48
49
50
51
52
53
54
55
56
57
58
59
60
61
62
63
64
65

313 vegetation patches. Edge density, an indicator of linear configuration of green space along the
314 streets, appears to be large on southwest and northeast parts of the study site. The spatial
315 distribution patterns of patch density and edge density are similar suggesting there exists some
316 degree of correlation between these two variables.

317 Insert Figure 3 here

318
319 Two dimensional scatter plots between LST and landscape metrics are shown in Fig. 4. There
320 seems to be a negative linear relationship between LST and both vegetation fraction and edge
321 density. However, these relationships do not seem to be statistically significant enough ($R^2 <$
322 0.32 in all cases) to obtain meaningful conclusions. That is why other measures may play an
323 important role. However, some useful information can be extracted. It is interesting to note that
324 patch density and edge density are correlated variables but demonstrates very different degrees
325 of effects on LST. The results imply that edge density has more deterministic effects on LST
326 than the patch density. One may expect that plantation of street trees evenly distributed in the
327 urban area may be an effective way of reducing urban heat island effects, therefore, energy
328 consumption as opposed to establishing dense patches of green space in discrete locations.

329
330 Insert Figure 4 here

331
332 Table 3 shows the normalized mutual information analysis between the LST and landscape
333 metrics calculated using Eq. (15). It is evident that the compositional and spatial configuration of
334 urban green space can affect the LST to a certain degree. When these two major categories of
335 green space pattern are taken into account separately, it seems the compositional green space

1
2
3
4 336 pattern has slightly larger effect on LST than configurational factors. Meanwhile, the
5
6
7 337 configurational green space patterns do have relatively strong effect but not as strong as
8
9 338 compositional green space pattern. The mutual information value was largest when all three
10
11 339 landscape metrics were considered in order to see the effect on the LST. This is expected since
12
13
14 340 each of the landscape metrics does have some level of causal interactions with LST change, and
15
16 341 the effects could constructively interfere each other. Combination of any two or three of the
17
18
19 342 landscape metrics had a higher impact on LST than that of a single variable. The joint effect of
20
21 343 (*PLAND*, *PD*) was slightly better in magnitude than the effect of (*PLAND*, *ED*) on LST,
22
23
24 344 confirming the stronger correlation between edge density and LST as shown in Fig. 4. However,
25
26 345 the mutual information value between (*ED*, *PD*) and LST was larger than of the (*PLAND*, *PD*)
27
28
29 346 and (*PLAND*, *ED*), which might be attributed to the fact that 1) patch density and edge density is
30
31 347 more determinative factors that elicits LST, and 2) there exist correlations between patch density
32
33 348 and edge density.

35
36 349 Insert Table 3 here
37
38

39 350 **5. Discussion**
40
41 351

42
43
44 352 The results of this study showed that *PLAND* was correlated with LST with statistical
45
46 353 significance. This is consistent with a number of previous studies, which demonstrated negative
47
48
49 354 correlations between LST and the abundance of green space measured by Normalized Difference
50
51 355 Vegetation Index (Buyantuyev and Wu, 2010; Chen et al., 2006), fraction of vegetation (Weng et
52
53
54 356 al., 2004), percent cover of LCLU (e.g., Forest, Grass, Cropland, etc.) (Weng et al., 2006; Zhou
55
56 357 et al., 2011), or *PLAND* (Li et al., 2012). Trees and other plants help cool the environment,
57
58 358 making green space a simple and effective way to mitigate urban heat island effects. Green
59
60
61
62
63
64
65

1
2
3
4 359 spaces lower surface and air temperatures by evapotranspiration due to its lower thermal inertia
5
6
7 360 compared to impervious surfaces and bare soils (Hamada and Ohta, 2010; Lambin and Ehrlich,
8
9 361 1996; Weng et al., 2004); by providing shade that prevents land surfaces from direct heating
10
11 362 from sunlight (Zhou et al., 2011). Concerning the configurational metrics, the PD and ED were
12
13
14 363 less correlated with LST than PLAND. The normalized mutual information analysis also showed
15
16 364 that there was less dependence between the LST with individual PD and ED, which is still
17
18
19 365 smaller than the dependence between the PLAND and LST. This indicates that the increase of
20
21 366 patch density leads to a decrease in mean patch size resulting in a general increase in total patch
22
23
24 367 edges. Therefore, the effects of the increase in patch density on LST can be explained by both a
25
26 368 decrease in mean patch size and increase in patch edges. The decrease in mean patch size may
27
28
29 369 increase LST because a larger, continuous green space produces stronger cool island effects than
30
31 370 that of several small pieces of green space even if whose total area equals to the area of the
32
33 371 continuous green space (Cao et al., 2010; Li et al., 2012; Zhang et al., 2009). In contrast, the
34
35
36 372 increase of total patch edges may enhance energy flow and exchange between green space and
37
38 373 its surrounding areas, and provide more shade for surrounding surfaces, which lead to the
39
40
41 374 decrease of LST (Zhou et al., 2011).

42
43 375
44
45
46 376 As far as the each landscape metric is concerned individually, the highest normalized
47
48 377 mutual information measure was found with the PLAND (0.71). The implication from this
49
50
51 378 observation is that the composition of green space was more important than the configuration of
52
53 379 green space in reducing UHI effects, which is consistent with previous findings (Li et al., 2012;
54
55 380 Zhou et al., 2011). However, our results also showed that ED and PD together were the most
56
57
58 381 deterministic factors of LST than the unique effects of a single variable or the joint effects

1
2
3
4
5
6
7
8
9
10
11
12
13
14
15
16
17
18
19
20
21
22
23
24
25
26
27
28
29
30
31
32
33
34
35
36
37
38
39
40
41
42
43
44
45
46
47
48
49
50
51
52
53
54
55
56
57
58
59
60
61
62
63
64
65

382 PLAND and PD or PLAND and ED. Normalized mutual information measure between LST and
383 PLAND and ED, PLAND and PD and ED and PD were 0.7679, 0.7650 and 0.7832, respectively.
384 A combination of the three factors PLAND, PD and ED explained much of the variance of LST
385 with a normalized mutual information measure of 0.8694. This is because the composition and
386 configuration of green space are constructively interrelated.

387 Many of the results from this study regarding to the relationships between the green space
388 and LST were expected as reported in a number of publications (Connors et al., 2013; Hamada
389 and Ohta, 2010; Li et al., 2011; Weng et al., 2004). Traditionally, increasing the green space by
390 planting more trees has been emphasized in urban planning (Rizwan et al., 2008a; Zhou et al.,
391 2011). While confirming the fact that the increase in green space can significantly mitigate UHI
392 effects, our results showed that configuration of green space as expressed by the joint effect of
393 PD and ED is the most deterministic metric that affects LST. Optimizing the configuration of
394 green space which increases the PD and ED should be highlighted to mitigate UHI effects. These
395 results have important implications for green space management, particularly in rapidly
396 urbanizing arid regions as in our case study, where both water resources and available land area
397 for increased green space is extremely limited.

398 Under changing climate, arid regions are likely to become even drier, while wet areas
399 tend to get wetter in response to observed global warming (Durack et al., 2012) as indicated by
400 increasing surface temperature. Expanding the urban green space is a rational approach for
401 adapting to climate change. At the same time, it can contribute to the sustainable development of
402 urban areas. However, it may compete with other socio-economic interests that also require
403 space. Therefore, in order to determine a proper balance between the sustainable development
404 and urban green space increase, urban planners should work on optimizing the configuration of

1
2
3
4
5
6
7
8
9
10
11
12
13
14
15
16
17
18
19
20
21
22
23
24
25
26
27
28
29
30
31
32
33
34
35
36
37
38
39
40
41
42
43
44
45
46
47
48
49
50
51
52
53
54
55
56
57
58
59
60
61
62
63
64
65

405 green space patches in selected areas by increasing the size of existing green space patches rather
406 than building new smaller patches. In the arid Northwestern China, where temperatures are
407 already high and water resources are limited, the outcome of this study can support decisions
408 about sustainable urban design and development, which will help mitigating the effects of future
409 climate, and benefit human wellbeing by improving water and energy use efficiency.

6. Conclusion

411
412 Taking the urban area of the oasis city of Aksu area as an example, this study
413 quantitatively examined the effects of spatial composition and configuration of green space on
414 land surface temperature (LST). Normalized mutual information measure was used to quantify
415 the relationship between LST and landscape metrics including percentage of landscape
416 (PLAND), edge density (ED) and patch density (PD). Our results showed that 1) both the
417 composition and configuration of green space elicits urban heat island; 2) joint effects of any two
418 combinations of the metrics was larger than the effect of a single metric; 3) ED and PD
419 combined was the most deterministic factor of LST than the unique effects of a single variable or
420 the joint effects PLAND and PD or PLAND and ED; 4) optimizing the configuration of green
421 space which increases the PD and ED should be prioritized in sustainable urban planning and
422 development to mitigate urban heat island effects.

423 Water scarcity is the major limiting factor of anthropogenic activities in arid and semi-
424 arid regions. Specifically, the increase of green space cover is restricted by water availability.
425 Our results suggested that by increasing patch and edge density of the green space, the thermal
426 environment in the City of Aksu can be further improved without expanding the percentage of
427 landscape (PLAND). In arid and semi-arid regions, where temperatures are already high and

1
2
3
4
5
6
7
8
9
10
11
12
13
14
15
16
17
18
19
20
21
22
23
24
25
26
27
28
29
30
31
32
33
34
35
36
37
38
39
40
41
42
43
44
45
46
47
48
49
50
51
52
53
54
55
56
57
58
59
60
61
62
63
64
65

428 water resources are limited, the outcome of this study may provide climate change adaptation
429 and mitigation benefits by reducing greenhouse gas emissions and energy demand for the
430 cooling of buildings.

431

432 **Acknowledgments**

433

434 The first author would like to express his gratitude to the European Commission and Erasmus
435 Mundus Consortium for their important scholarship for master students. We acknowledge the
436 National Natural Science Foundation of China (#s: 31270742, U1138303, 41130531, 41361016),
437 Sino-German joint research project SuMaRiO (01LL0918C), Research Foundation of Xinjiang
438 University (BS120116 and XY110117) and Education Department of Xinjiang
439 Uygur Autonomous Region (XJEDU2011S07) for financially supporting this work. Finally, we
440 also extend our gratitude to the anonymous reviewers of this manuscript for their helpful
441 suggestions.

442 **References**

443

444 Alberti, M., 2005. The effects of urban patterns on ecosystem function. *International regional*
445 *science review* 28, 168-192.
446 Allaby, M., 2008. *A Dictionary of Earth Sciences*, Third ed. Oxford University Press Inc., New
447 York, pp: 460
448 Arnfield, A.J., 2003. Two decades of urban climate research: a review of turbulence, exchanges
449 of energy and water, and the urban heat island. *International Journal of Climatology* 23,
450 1-26.

1
2
3
4
5
6
7
8
9
10
11
12
13
14
15
16
17
18
19
20
21
22
23
24
25
26
27
28
29
30
31
32
33
34
35
36
37
38
39
40
41
42
43
44
45
46
47
48
49
50
51
52
53
54
55
56
57
58
59
60
61
62
63
64
65

451 Baker, L.A., Brazel, A.J., Westerhoff, P., 2004. Environmental consequences of rapid
452 urbanization in warm, arid lands: case study of Phoenix, Arizona (USA). In: Marchettini
453 N, Brebbia C, Tiezzi E, Wadhwa LC (eds) The sustainable city III, (Proceedings of the
454 Sienna Conference, held June 2004), Advances in Architecture Series, WIT Press,
455 Boston.

456 Bowler, D.E., Buyung-Ali, L., Knight, T.M., Pullin, A.S., 2010. Urban greening to cool towns
457 and cities: A systematic review of the empirical evidence. *Landscape and Urban Planning*
458 97, 147-155.

459 Buyantuyev, A., Wu, J., 2010. Urban heat islands and landscape heterogeneity: linking
460 spatiotemporal variations in surface temperatures to land-cover and socioeconomic
461 patterns. *Landscape ecology* 25, 17-33.

462 Cao, X., Onishi, A., Chen, J., Imura, H., 2010. Quantifying the cool island intensity of urban
463 parks using ASTER and IKONOS data. *Landscape and Urban Planning* 96, 224-231.

464 Carlson, T.N., Ripley, D.A., 1997. On the relation between NDVI, fractional vegetation cover,
465 and leaf area index. *Remote Sensing of Environment* 62, 241-252.

466 Chen, X.L., Zhao, H.M., Li, P.X., Yin, Z.Y., 2006. Remote sensing image-based analysis of the
467 relationship between urban heat island and land use/cover changes. *Remote Sensing of*
468 *Environment* 104, 133-146.

469 Connors, J.P., Galletti, C.S., Chow, W.T.L., 2013. Landscape configuration and urban heat
470 island effects: assessing the relationship between landscape characteristics and land
471 surface temperature in Phoenix, Arizona. *Landscape Ecology*, 28, 271-283.

472 Cover, T., Thomas, J., 1991. *Elements of Information Theory*. Wiley-Interscience.

1
2
3
4
5
6
7
8
9
10
11
12
13
14
15
16
17
18
19
20
21
22
23
24
25
26
27
28
29
30
31
32
33
34
35
36
37
38
39
40
41
42
43
44
45
46
47
48
49
50
51
52
53
54
55
56
57
58
59
60
61
62
63
64
65

473 Cui, Y.Y., de Foy, B., 2012. Seasonal Variations of the Urban Heat Island at the surface and the
474 near-surface and reductions due to urban vegetation in Mexico City. *Journal of Applied
475 Meteorology and Climatology*, 51, 855–868.

476 Dousset, B., Gourmelon, F., 2003. Satellite multi-sensor data analysis of urban surface
477 temperatures and landcover. *ISPRS Journal of Photogrammetry and Remote Sensing* 58,
478 43-54.

479 Durack, P.J., Wijffels, S.E., Matear, R.J., 2012. Ocean Salinities Reveal Strong Global Water
480 Cycle Intensification During 1950 to 2000. *Science* 336, 455-458.

481 Fan, P., Qi, J., 2010. Assessing the sustainability of major cities in China. *Sustainability Science*,
482 5, 51-68.

483 Feizizadeh, B., Blaschke, T., 2013. Examining urban heat island relations to land use and air
484 pollution: multiple endmember spectral mixture analysis for thermal remote sensing.
485 *IEEE Journal of Selected Topics in Applied Earth Observations and Remote Sensing*, 6,
486 1749-1756.

487 Gustafson, E.J., 1998. Quantifying landscape spatial pattern: What is the state of the art?
488 *Ecosystems* 1, 143-156.

489 Halik, W., Mamat, A., Dang, J.H., Deng, B.S.H., Tiyyip, T., 2013. Suitability analysis of human
490 settlement environment within the Tarim Basin in Northwestern China. *Quaternary
491 International*, 311, 175-180.

492 Hamada, S., Ohta, T., 2010. Seasonal variations in the cooling effect of urban green areas on
493 surrounding urban areas. *Urban forestry & urban greening* 9, 15-24.

494 Hamdi, R., Schayes, G., 2007. Sensitivity study of the urban heat island intensity to urban
495 characteristics. *International Journal of Climatology* 28, 973-982.

1
2
3
4
5
6
7
8
9
10
11
12
13
14
15
16
17
18
19
20
21
22
23
24
25
26
27
28
29
30
31
32
33
34
35
36
37
38
39
40
41
42
43
44
45
46
47
48
49
50
51
52
53
54
55
56
57
58
59
60
61
62
63
64
65

496 Honjo, T., Takakura, T., 1991. Simulation of thermal effects of urban green areas on their
497 surrounding areas. *Energy and Buildings* 15, 443-446.

498 Howard, L., 1818. *The climate of London, deduced from Meteorological observations, made at*
499 *different places in the neighbourhood of the metropolis, vol. 2*, London, 1818-20.

500 Huang, G., Zhou, W., Cadenasso, M.L., 2011. Is everyone hot in the city? Spatial pattern of land
501 surface temperatures, land cover and neighborhood socioeconomic characteristics in
502 Baltimore, MD. *Journal of Environmental Management*, 92,1753-1759.

503 Imhoff, M.L., Zhang, P., Wolfe, R.E., Bounoua, L., 2010. Remote sensing of the urban heat
504 island effect across biomes in the continental USA. *Remote Sensing of Environment*
505 114, 504-513.

506 James, W., 2002. Green roads: research into permeable pavers. *Stormwater* 3, 48-40.

507 Lai, L.-W., Cheng, W.-L., 2009. Air quality influenced by urban heat island coupled with
508 synoptic weather patterns. *Science of The Total Environment* 407, 2724-2733.

509 Lambin, E., Ehrlich, D., 1996. The surface temperature-vegetation index space for land cover
510 and land-cover change analysis. *International Journal of Remote Sensing* 17, 463-487.

511 Lee, S.-W., Hwang, S.-J., Lee, S.-B., Hwang, H.-S., Sung, H.-C., 2009. Landscape ecological
512 approach to the relationships of land use patterns in watersheds to water quality
513 characteristics. *Landscape and Urban Planning* 92, 80-89.

514 Li, H., Reynolds, J.F., 1993. A new contagion index to quantify spatial patterns of landscapes.
515 *Landscape ecology* 8, 155-162.

516 Li, H., Wu, J., 2004. Use and misuse of landscape indices. *Landscape ecology* 19, 389-399.

1
2
3
4 517 Li, J., Song, C., Cao, L., Zhu, F., Meng, X., Wu, J., 2011. Impacts of landscape structure on
5
6 518 surface urban heat islands: A case study of Shanghai, China. *Remote Sensing of*
7
8
9 519 *Environment* 115, 3249-3263.
10
11 520 Li, X., Zhou, W., Ouyang, Z., Xu, W., Zheng, H., 2012. Spatial pattern of greenspace affects
12
13
14 521 land surface temperature: evidence from the heavily urbanized Beijing metropolitan area,
15
16 522 China. *Landscape Ecology*, 27, 887-898.
17
18
19 523 Li, X., Zhou W., Ouyang, Z., 2013. Relationship between land surface temperature and spatial
20
21 524 pattern of greenspace: What are the effects of spatial resolution? *Landscape and Urban*
22
23 525 *Planning*, 114, 1-8.
24
25
26 526 Liu, G., Kurban, A., Duan, H., Halik, Ü., Ablekim, A., Zhang, L. Desert riparian forest
27
28 527 colonization in the lower reaches of Tarim River based on remote sensing analysis.
29
30 528 *Environmental Earth Sciences*, DOI: 10.1007/s12665-013-2850-9.
31
32
33 529 Liu, H., Weng, Q., 2008. Seasonal variations in the relationship between landscape pattern and
34
35 530 land surface temperature in Indianapolis, USA. *Environmental Monitoring Assessment*,
36
37 531 144, 199-219.
38
39
40 532 Mcgarigal, K., Cushman, S., Neel, M., Ene, E., 2002. FRAGSTATS: spatial pattern analysis
41
42 533 program for categorical maps.
43
44
45 534 McGarigal, K., Marks, B.J., 1995. Spatial pattern analysis program for quantifying landscape
46
47 535 structure. Gen. Tech. Rep. PNW-GTR-351. US Department of Agriculture, Forest
48
49 536 Service, Pacific Northwest Research Station.
50
51
52 537 Niemelä, J., 1999. Ecology and urban planning. *Biodiversity and conservation* 8, 119-131.
53
54
55 538 Patz, J.A., Campbell-Lendrum, D., Holloway, T., Foley, J.A., 2005. Impact of regional climate
56
57 539 change on human health. *Nature* 438, 310-317.
58
59
60
61
62
63
64
65

1
2
3
4 540 Press, W.H., Flannery, B.P., Teukolsky, S.A., Vetterling, W.T., 1990. Numerical recipes.
5
6
7 541 Cambridge Univ Press.
8
9 542 Pu, R., Gong, P., Michishita, R., Sasagawa, T., 2006. Assessment of multi-resolution and multi-
10
11 543 sensor data for urban surface temperature retrieval. Remote Sensing of Environment 104,
12
13 544 211-225.
14
15
16 545 Qin, Z.-h., Karnieli, A., Berliner, P., 2001. A mono-window algorithm for retrieving land surface
17
18 546 temperature from Landsat TM data and its application to the Israel-Egypt border region.
19
20
21 547 International Journal of Remote Sensing 22, 3719-3746.
22
23
24 548 Riitters, K.H., O'Neill, R., Hunsaker, C., Wickham, J.D., Yankee, D., Timmins, S., Jones, K.,
25
26 549 Jackson, B., 1995. A factor analysis of landscape pattern and structure metrics.
27
28 550 Landscape ecology 10, 23-39.
29
30
31 551 Riva-Murray, K., Riemann, R., Murdoch, P., Fischer, J.M., Brightbill, R., 2010. Landscape
32
33 552 characteristics affecting streams in urbanizing regions of the Delaware River Basin (New
34
35 553 Jersey, New York, and Pennsylvania, US). Landscape ecology 25, 1489-1503.
36
37
38 554 Rizwan, A.M., Dennis, L.Y., Liu, C., 2008a. A review on the generation, determination and
39
40 555 mitigation of Urban Heat Island. Journal of Environmental Sciences 20, 120-128.
41
42
43 556 Rizwan, A.M., Dennis, L.Y.C., Liu, C., 2008b. A review on the generation, determination and
44
45 557 mitigation of Urban Heat Island. Journal of Environmental Sciences 20, 120-128.
46
47
48 558 Sarrat, C., Lemonsu, A., Masson, V., Guedalia, D., 2006. Impact of urban heat island on regional
49
50 559 atmospheric pollution. Atmospheric Environment 40, 1743-1758.
51
52
53 560 Sobrino, J.A., Jiménez-Muñoz, J.C., Paolini, L., 2004. Land surface temperature retrieval from
54
55 561 LANDSAT TM 5. Remote Sensing of Environment 90, 434-440.
56
57
58
59
60
61
62
63
64
65

1
2
3
4
5
6
7
8
9
10
11
12
13
14
15
16
17
18
19
20
21
22
23
24
25
26
27
28
29
30
31
32
33
34
35
36
37
38
39
40
41
42
43
44
45
46
47
48
49
50
51
52
53
54
55
56
57
58
59
60
61
62
63
64
65

562 Sridhar, D.V., Bartlett, E.B., Seagrave, R.C., 1998. Information theoretic subset selection for
563 neural network models. *Computers & chemical engineering* 22, 613-626.

564 Strehl, A., Ghosh, J., 2003. Cluster ensembles---a knowledge reuse framework for combining
565 multiple partitions. *The Journal of Machine Learning Research* 3, 583-617.

566 Taha, H., 1997. Urban climates and heat islands: albedo, evapotranspiration, and anthropogenic
567 heat. *Energy and buildings* 25, 99-103.

568 Tran, H., Uchihama, D., Ochi, S., Yasuoka, Y., 2006. Assessment with satellite data of the urban
569 heat island effects in Asian mega cities. *International Journal of Applied Earth
570 Observation and Geoinformation* 8, 34-48.

571 Turner, M.G., 2005. Landscape ecology: what is the state of the science? *Annual Review of
572 Ecology, Evolution, and Systematics*, 319-344.

573 Turner, M.G., O'Neill, R.V., Gardner, R.H., Milne, B.T., 1989. Effects of changing spatial scale
574 on the analysis of landscape pattern. *Landscape ecology* 3, 153-162.

575 Unger, J., 2004. Intra-urban relationship between surface geometry and urban heat island: review
576 and new approach. *Climate research* 27, 253-264.

577 Voogt, J.A., Oke, T., 1998. Effects of urban surface geometry on remotely-sensed surface
578 temperature. *International Journal of Remote Sensing* 19, 895-920.

579 Voogt, J.A., Oke, T.R., 2003. Thermal remote sensing of urban climates. *Remote sensing of
580 Environment* 86, 370-384.

581 Solecki, W.D., Rosenzweig, C., Parshall, L., Pope, G., Clark, M., Cox, J., Wiencke, M., 2005.
582 Mitigation of the heat island effect in urban New Jersey. *Global Environmental Change
583 Part B: Environmental Hazards*, 6, 39-49.

584 Webb, A.R., 2002. *Statistical pattern recognition*. Wiley.

1
2
3
4 585 Weng, Q., 2001. A remote sensing? GIS evaluation of urban expansion and its impact on surface
5
6 586 temperature in the Zhujiang Delta, China. *International Journal of Remote Sensing* 22,
7
8
9 587 1999-2014.
10
11 588 Weng, Q., 2009. Thermal infrared remote sensing for urban climate and environmental studies:
12
13
14 589 Methods, applications, and trends. *ISPRS Journal of Photogrammetry and Remote*
15
16 590 *Sensing* 64, 335-344.
17
18
19 591 Weng, Q., Liu, H., Lu, D., 2007. Assessing the effects of land use and land cover patterns on
20
21 592 thermal conditions using landscape metrics in city of Indianapolis, United States. *Urban*
22
23
24 593 *Ecosystems* 10, 203-219.
25
26 594 Weng, Q., Lu, D., Liang, B., 2006. Urban surface biophysical descriptors and land surface
27
28 595 temperature variations. *Photogrammetric Engineering & Remote Sensing* 72, 1275-1286.
29
30
31 596 Weng, Q., Lu, D., Schubring, J., 2004. Estimation of land surface temperature–vegetation
32
33 597 abundance relationship for urban heat island studies. *Remote sensing of Environment* 89,
34
35
36 598 467-483.
37
38 599 Weng, Q., Yang, S., 2006. Urban Air Pollution Patterns, Land Use, and Thermal Landscape: An
39
40 600 Examination of the Linkage Using GIS. *Environ Monit Assess* 117, 463-489.
41
42
43 601 Wu, C-D., Lung, S-C. C., Jan, J-F., 2013. Development of a 3-D urbanization index using digital
44
45 602 terrain models for surface urban heat island effects. *ISPRS Journal of Photogrammetry*
46
47
48 603 and *Remote Sensing*, 81, 1-11.
49
50 604 Wu, J., 2000. *Landscape ecology: pattern, process, scale and hierarchy*. Beijing: Higher
51
52 605 Education Press 13, 121-123.
53
54
55 606 Wu, J., Shen, W., Sun, W., Tueller, P.T., 2002. Empirical patterns of the effects of changing
56
57 607 scale on landscape metrics. *Landscape Ecology* 17, 761-782.
58
59
60
61
62
63
64
65

1
2
3
4
5
6
7
8
9
10
11
12
13
14
15
16
17
18
19
20
21
22
23
24
25
26
27
28
29
30
31
32
33
34
35
36
37
38
39
40
41
42
43
44
45
46
47
48
49
50
51
52
53
54
55
56
57
58
59
60
61
62
63
64
65

608 Xian, G., Crane, M., 2006. An analysis of urban thermal characteristics and associated land
609 cover in Tampa Bay and Las Vegas using Landsat satellite data. *Remote Sensing of*
610 *Environment* 104, 147-156.

611 Yokohari, M., Brown, R.D., Kato, Y., Moriyama, H., 1997. Effects of paddy fields on
612 summertime air and surface temperatures in urban fringe areas of Tokyo, Japan.
613 *Landscape and urban planning* 38, 1-11.

614 Zhang, X., Zhong, T., Feng, X., Wang, K., 2009. Estimation of the relationship between
615 vegetation patches and urban land surface temperature with remote sensing. *International*
616 *Journal of Remote Sensing* 30, 2105-2118.

617 Zhao, C., Fu, G., Liu, X., Fu, F., 2011. Urban planning indicators, morphology and climate
618 indicators: A case study for a north-south transect of Beijing, China. *Building and*
619 *Environment* 46, 1174-1183.

620 Zhou, W., Huang, G., Cadenasso, M.L., 2011. Does spatial configuration matter? Understanding
621 the effects of land cover pattern on land surface temperature in urban landscapes.
622 *Landscape and Urban Planning* 102, 54-63.

623
624
625
626
627
628
629

1
2
3
4
5
6
7
8
9
10
11
12
13
14
15
16
17
18
19
20
21
22
23
24
25
26
27
28
29
30
31
32
33
34
35
36
37
38
39
40
41
42
43
44
45
46
47
48
49
50
51
52
53
54
55
56
57
58
59
60
61
62
63
64
65

Tables:

Table 1 Accuracy assessment of the urban green space classification map

Table 2 Landscape metrics used in this study(Mcgarigal et al., 2002)

Table 3 Normalized mutual information results of compositional configuration of green space and landscape metrics

Figures:

Fig. 1. Location map of the study area showing overview map of China (top - left corner) and the Xinjiang Uyghur Autonomous Region (bottom-left corner).

Fig. 2. Green space and LST maps for the downtown are Aksu city: (a) green space map, and (b) LST map with units of Kelvin

Fig. 3. Grid map of urban green space metrics (a) Percent cover of green space (b) Patch density (c) Edge density

Fig. 4. Scatter plot of LST with PLAND, PD and ED

Figure 1
Click here to download high resolution image

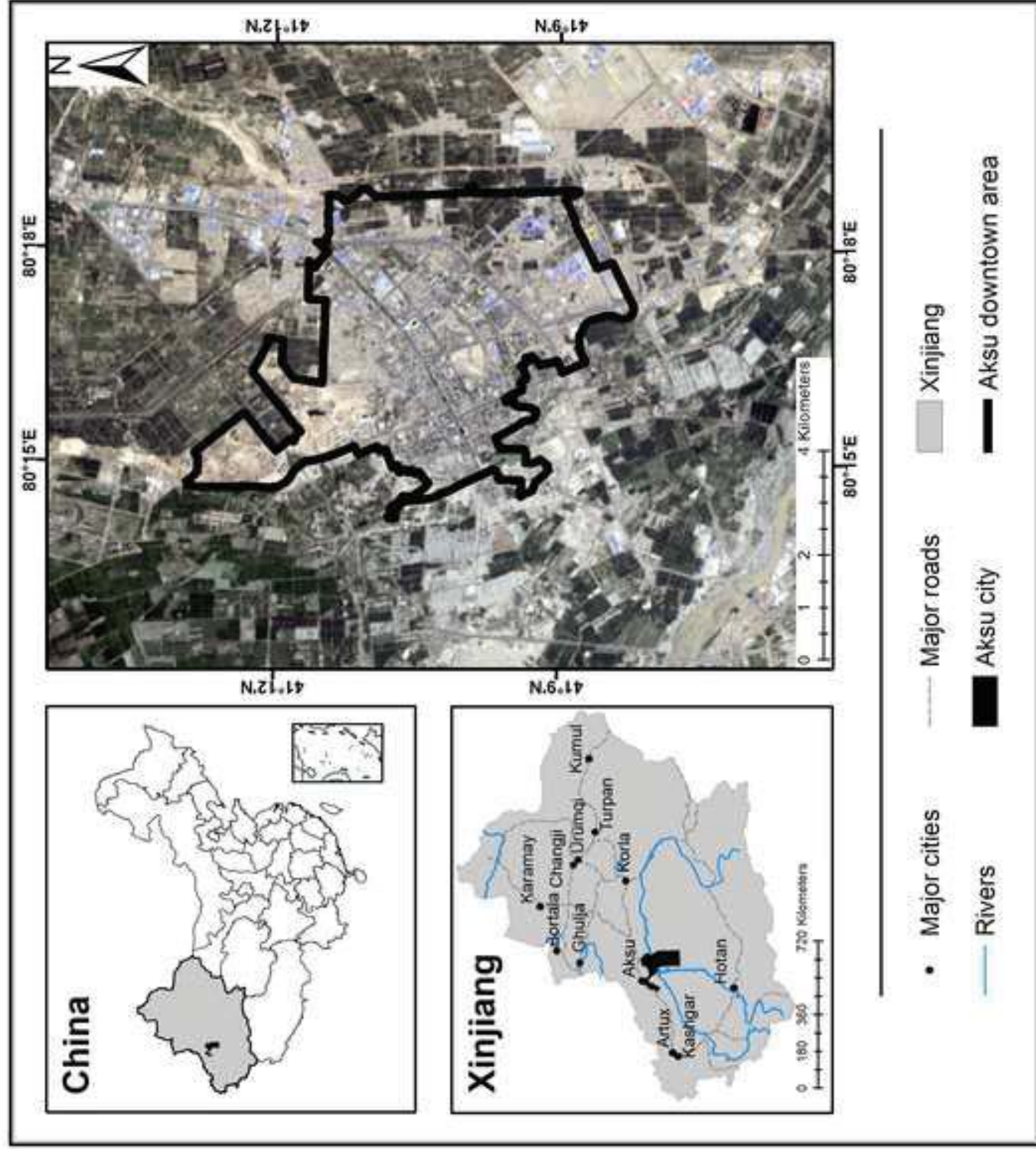


Figure 2
[Click here to download high resolution image](#)

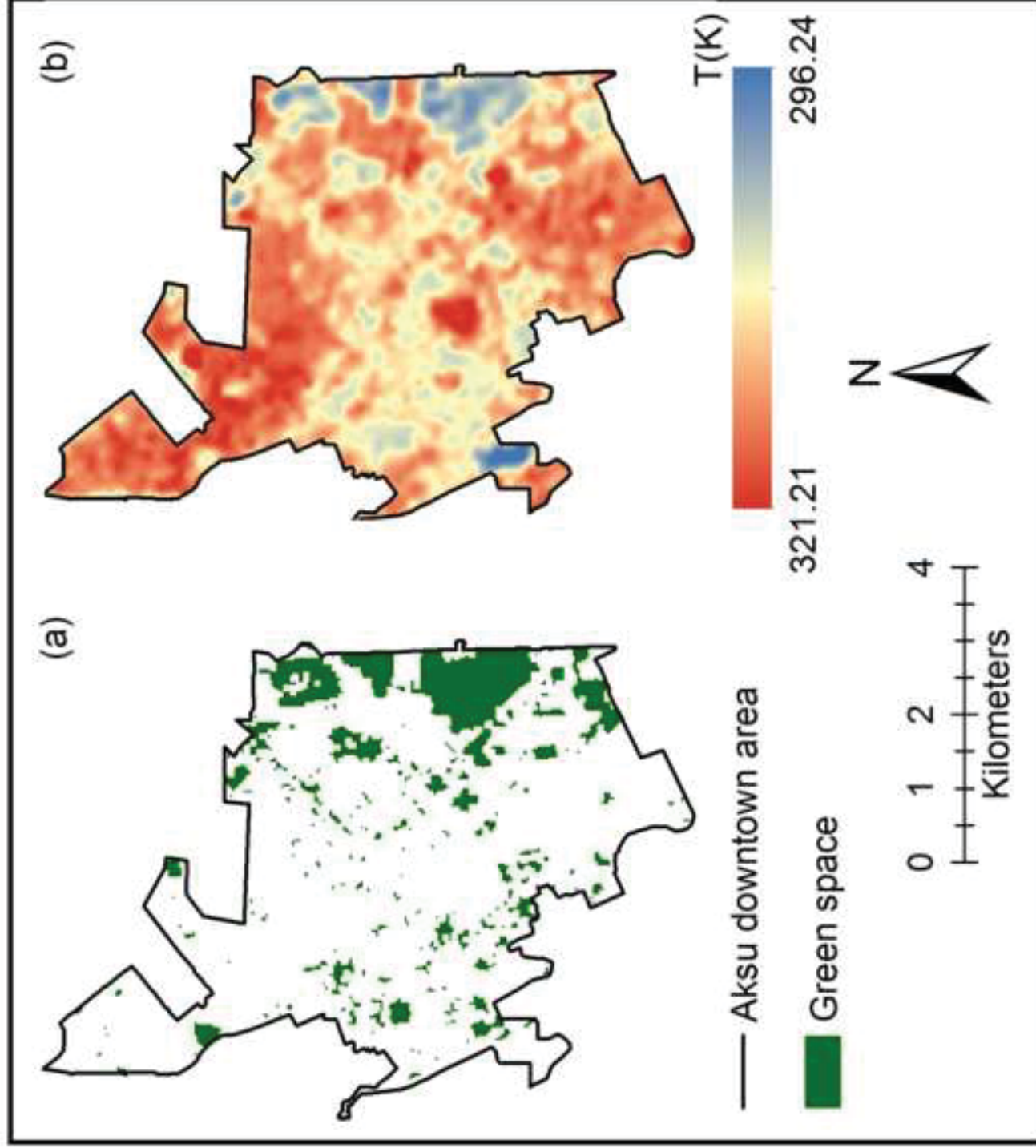


Figure 3
[Click here to download high resolution image](#)

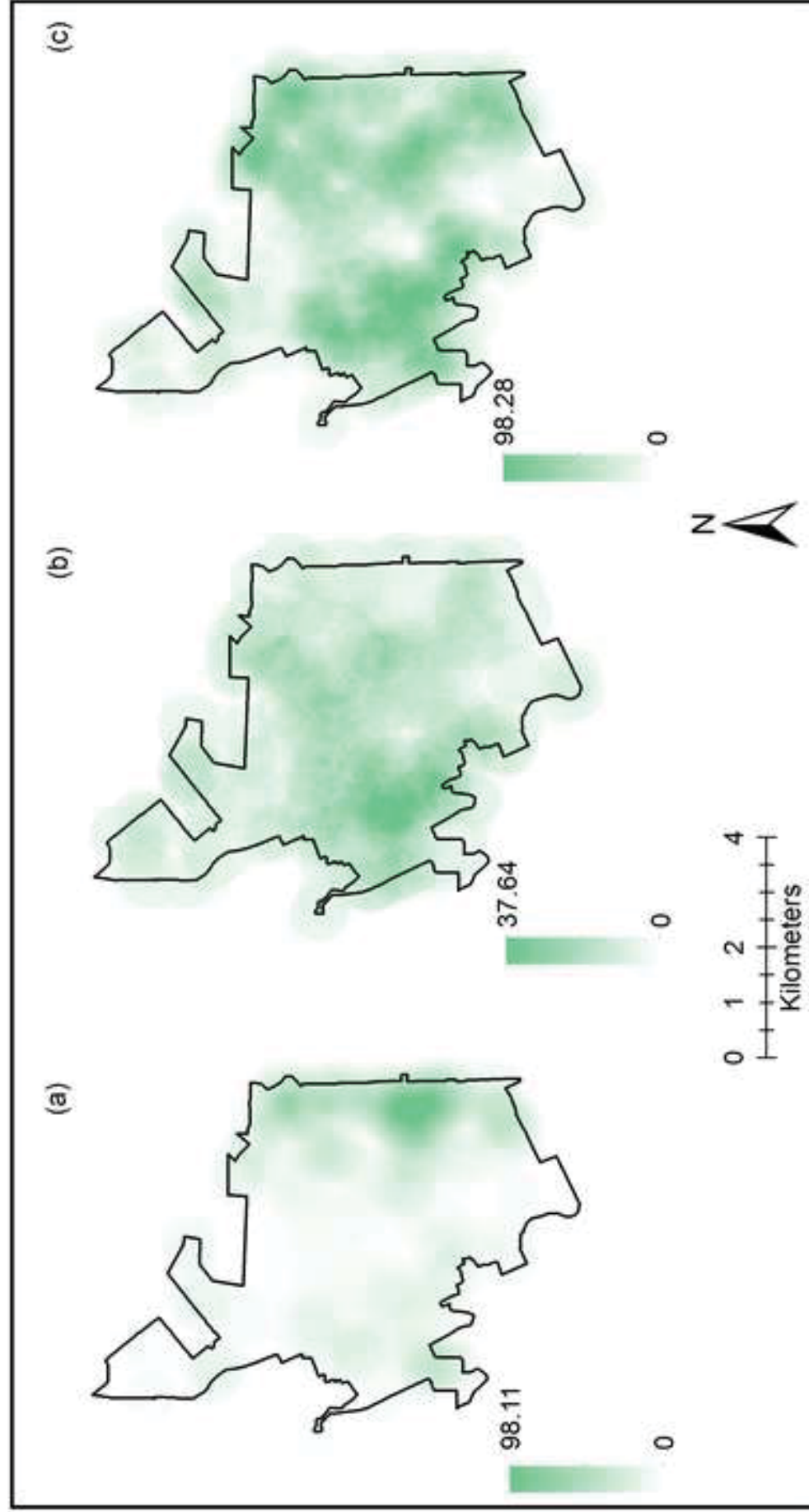


Figure 4
[Click here to download high resolution image](#)

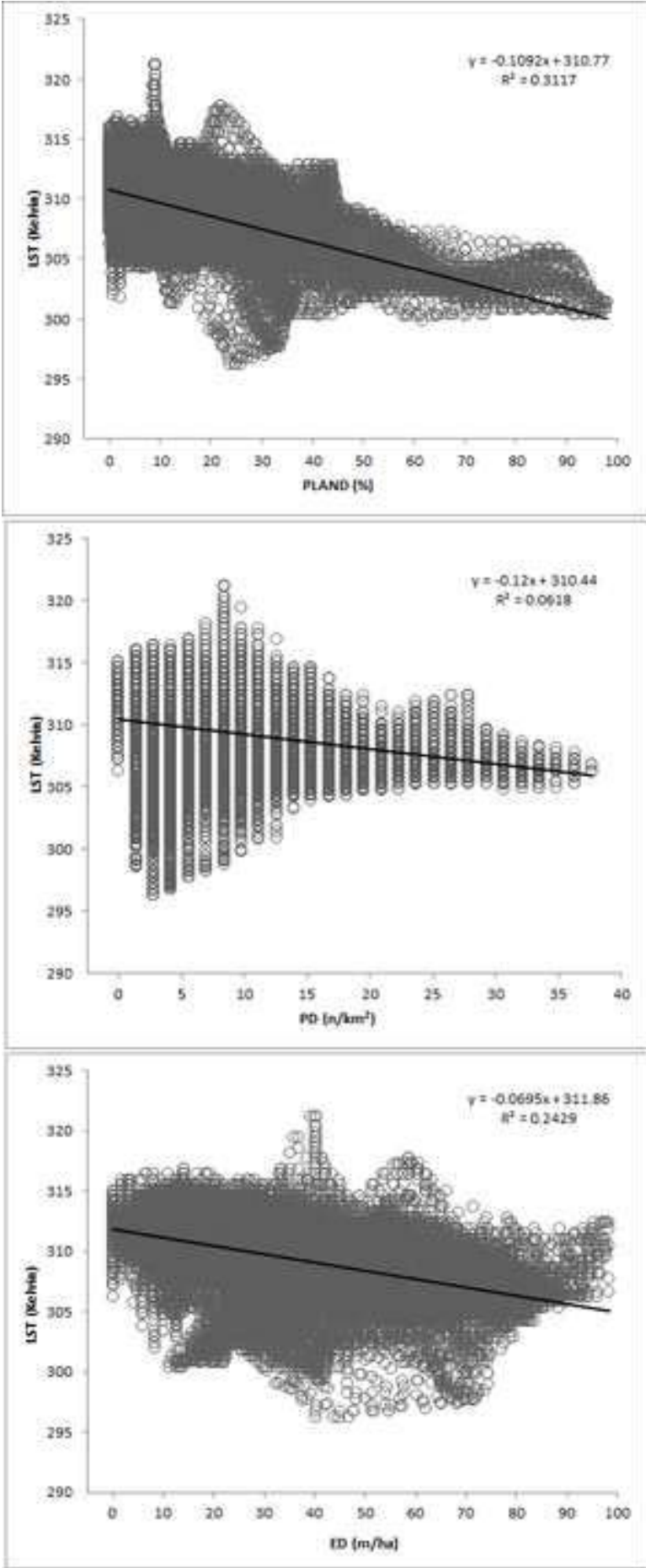


Table 1

[Click here to download Table: Table 1 Accuracy assessment of the urban green space derived map.docx](#)

Table 1 Accuracy assessment of the urban green space classification map.

	Reference data (Pixels)				Total	User's accuracy (%)
	Urban green space	Residential area	Construction site	Water body		
Urban green space	231	6	2	2	241	95.9
Residential area	0	170	15	2	187	90.9
Construction site	1	53	148	2	202	73.3
Water body	0	11	0	99	110	90.0
Total	232	240	165	103	740	
Producer's accuracy (%)	99.6	70.8	89.7	96.1		
Overall Accuracy (%)	87.6					
Kappa coefficient	0.83					

Table 2 Landscape metrics used in this study(Mcgarigal et al., 2002)

Metrics (abbreviation)	Calculation and description
<i>Compositional</i>	
Percentage of Landscape (PLAND)	$100/A \times \sum_{i=1}^n a_i$ Proportional abundance of green space in the landscape (%)
<i>Configurational</i>	
Patch density(PD)	$n/A \times 10^6$ Number of green space patches divided by total landscape area (n/km ²)
Edge density(ED)	$10,000/A \times \sum_{i=1}^n e_i$ Total length (border not included) of all edge segments of green space per hectare (m/ha)

a_i area of patch i ; e_i length of edge (or perimeter) of patch i ; A landscape area; n number of patches

Table 3
[Click here to download Table: Table 3 Normalized mutual information results of compositional configuration of green space and](#)

Table 3 Normalized mutual information results of compositional configuration of green space and landscape metrics

C_{XY}		Normalized mutual information
X	Y	value
PLAND		0.7100
PD		0.6985
ED		0.7033
PLAND, PD	LST	0.7679
PLAND, ED		0.7650
PD, ED		0.7832
PLAND, PD,ED		0.8694